First publ. in: Environmental Science & Technology 41 (2007), 7, pp. 2609 -2616

Analytical and Functional Characterization of Microcystins [Asp^3]MC-RR and [Asp^3,Dhb^7]MC-RR: Consequences for Risk Assessment?

S. J. HOEGER,[†] D. SCHMID,[†,§] J. F. BLOM,[‡] B. ERNST,[†] AND D. R. DIETRICH*,[†]

Environmental Toxicology, University of Konstanz, Germany, and Limnological Station, Institute of Plant Biology, University of Zürich, Switzerland

The microcystin (MC) producing *P. rubescens* occurs in pre-alpine lakes and may impact fishery success, bathing, and raw water quality. *P. rubescens* extracts, characterized via LC-MS, contained the two MC-RR variants [Asp^3]MC-RR and [Asp^3,Dhb^7]MC-RR. The protein-phosphatase-inhibition assay (cPPIA with phosphatases 1 and 2A) in its capability to quantify [Asp^3]MC-RR, [Asp^3,Dhb^7]MC-RR, and MC-RR was compared to HPLC-DAD and anti-Adda-ELISA. The IC_{50} values (PP1 and PP2A) determined for MC-LR, MC-RR, and [Asp^3]MC-RR were in the same range (1.9−3.8 and 0.45−0.75 nM). A 50-fold higher concentration of [Asp^3,Dhb^7]MC-RR (29.8 nM) was necessary to inhibit the PP2A by 50%. The PP1-IC_{50} of [Asp^3,Dhb^7]MC-RR was 22-fold higher (56.4 nM) than those of the other MCs, suggesting that specific structural characteristics are responsible for its weaker PPI capacity. Western blots demonstrated that [Asp^3,Dhb^7]MC-RR does not covalently bind to PP1. [Asp^3,Dhb^7]MC-RR has comparable in vivo LD_{50} values to MC-RR, despite a far lower PP-inhibiting capacity, suggesting that toxicodynamic and toxicokinetic characteristics of [Asp^3,Dhb^7]MC-RR are responsible for its high in vivo toxicity. The data demonstrate that cPPIA analysis of [Asp^3,Dhb^7]MC-RR-containing samples prevent reliable MC determination and lead to underestimation of potential toxicity.

Introduction

Water blooms containing toxic cyanobacteria occur ubiquitously worldwide. These blooms may represent a hazard to humans and to the environment (*1*). A cyanobacterial genus well-known for its potential to produce toxins is the filamentous *Planktothrix*, frequently found in European lakes (*2*, *3*). In Lake Ammersee (Southern Germany), *P. rubescens* is one of the dominant planktonic species, and it regularly attains high densities and produces several microcystin congeners (MCs) (*2*, *4*, *5*). The principal structure of the approximately 80 different MCs is cyclo-(D-Ala^1-L-X^2-D-MAsp^3-L-Z^4-Adda^5-D-Glu^6-MDha^7), whereby MAsp^3 stands for erythro-β-methylaspartic acid, Adda for 4*E*,6*E*-3-amino-9-methoxy-2,6,8-trimethyl-10-phenyldeca-4,6-dienoic acid, and MDha^7 for *N*-methyldehydroalanine. X and Z represent two variable amino acids with 15 and 12 variations reported, respectively. Structural modifications are reported for the remaining amino acids; however, demethylation on MAsp, MDha, or Adda and/or esterification of glutamic acid and Z-configuration of Adda occur most frequently. Nodularins (NODs), toxic cyanobacterial pentapeptides with a similar principal structure, i.e., cyclo-(D-MAsp^1-L-Arg^2-Adda^3-D-Glu^4-MDhb^5), whereby MDhb^5 represents N-methyldehydrobutyric acid, are produced by the brackish water cyanobacterium *Nodularia spumigena* (*6*). Although the functional and ecological role(s) of MCs and NODs is unknown (*7*), it is beyond dispute that MCs and NODs are responsible for adverse health effects in humans and animals (*8*).

Following ingestion MCs and NODs are absorbed from the gastro-intestinal tract, reach the liver via the portal vein, and are actively taken up from the blood into hepatocytes via bile acid transporters (*9*). MCs and NODs are specific and highly effective inhibitors of the catalytic subunits of several serine/threonine protein-phosphatases (PP) (*10*). As a consequence of PP-inhibition, cellular phospho-proteins (e.g., micro- and intermediate-filaments, tau proteins, tumor suppressors, etc.) are hyperphosphorylated. Following acute intoxication, cytoskeletal protein hyperphosphorylation leads to disintegration of the cytoskeletal scaffold with subsequent apoptosis, necrosis, and finally, liver failure (*11*). In contrast, chronic exposure results in hepatocyte proliferation, most likely due to hyperphosphorylation of tumor suppressor proteins and, finally, in liver tumor promotion (reviewed in ref *8*). NODs may have tumor-initiating as well as promoting activity (*12*). Consequently, the International Agency for Cancer Research (IARC) classified MC-LR in the *2B* category, *probably carcinogenic to humans* (*13*).

Studies aimed at defining binding of MCs to PP1 and PP2A (*14*, *15*) reported that the MDha residue of MC-LR covalently binds to the cysteine-273 and cysteine-266 residues of PP1 and PP2A, respectively, although binding does not induce changes in MC-LR conformation (*16*). This was corroborated via crystallographic structure-analysis of the MC-LR-PP1 complex (*17*). In contrast, NOD does not covalently bind to protein-phosphatases (*15*, *18*). Moreover, the >10 Å distance between the β-carbon of the Mdhb residue and the sulfur atom of the Cys-273 side chain of the PP1-catalytic-subunit (*18*) most likely renders NOD incapable of covalent binding to PP1 and PP2A. Consequently, the electrophilic residue of the Mdhb moiety remains capable of interactions with various cellular reaction partners (e.g., DNA, proteins), therefore, explaining the carcinogenic nature of NOD.

Previous analyses of field samples containing MC-RR variants via PPIA and other detection methods provided evidence that the protein-phosphatase-inhibiting (PPI) capacity of MC-RR variants was not of the expected potency (*19*−*20*). To clarify which of the MC-RR variants are responsible for this lowered PPI capacity, two commonly produced demethylated MCs ([Asp^3]MC-RR and [Asp^3,Dhb^7]MC-RR) isolated from *P. rubescens* were characterized using HPLC-DAD, LC/MS, ELISA, PPIA, and immunoblotting techniques.

Materials and Methods

Sampling and Cultivation of Cyanobacteria. Two unialgal Lake Ammersee *P. rubescens* cultures were isolated from vertical seston samples (DS-129 and DS-29V, see the Sup-

* Corresponding author phone: +49 7531 88 3518; fax: +49 7531 88 3170; e-mail: daniel.dietrich@uni-konstanz.de.
[†] University of Konstanz.
[‡] University of Zürich.
[§] Current address: Department of Bioorganic Chemistry, Max Planck Institute for Chemical Ecology, Jena, Germany.

porting Information). DS-129, DS-29V, and axenic strain A7 (Lake Zürich) were grown as batch cultures in 50 mL conical flasks at 21 °C and a 16:8h light:dark cycle with ca. 40μE/m^{2}s from fluorescent tube lighting. Cells were harvested after 6 weeks of growth and stored at −20 °C. DS-29V, known to exclusively produce [Asp^3]MC-RR, was used to purify [Asp^3]-MC-RR. A7 was used to purify [Asp^3,Dhb^7]MC-RR.

Extraction and Purification. The extraction of MCs from strain A7 and DS-29V was carried out in triplicates with 70% MeOH with 15 min sonication (see the Supporting Information). After centrifugation (15 min, 3000*g*), supernatents were pooled, diluted to less than 10% MeOH, and purified by C_{18} solid-phase extraction. C_{18} SPE cartridges (International Sorbent Technology, Germany) were conditioned with 100% MeOH (15 mL) followed by an equilibration step with deionized water (15 mL). Following application of the cyanobacterial extracts, the cartridge was washed with deionized water (15 mL) and 10% MeOH (15 mL), and the toxin was subsequently eluted with 50 mL 100% MeOH. This methanolic fraction was dried under a gentle stream of nitrogen, resuspended in 100% MeOH, and finally diluted to 20% MeOH with purified water. Separation and purification of the MCs was performed on a C_{18} Grom-Sil 120 ODS-4, HE reversed phase column (11 μm particle size, 250 × 10 mm, Grom, Germany) using an isocratic 27% acetonitrile and 0.0135M ammonium acetate buffer (3 mL/min) as mobile phase (v/v). The HPLC system consisted of a pump solvent module model 125 and an autosampler model 507e (Beckman, Germany) coupled with a photodiode-array detector SPD-M10A (Shimadzu, Germany).

The methanolic (70%) extraction of MCs from strain DS-129 (5 mg DS-129 dw in 5 mL MeOH) was carried out in triplicates including sonication (15 min). The three supernatants were pooled after centrifugation (15 min, 3000*g*), diluted to less than 10% MeOH and purified by C_{18} solid-phase extraction as described above (Scheme 1).

Analysis. *RP-HPLC UV-DAD.* A C_{18} reversed-phase column (Grom-Sil 120 ODS-4 HE, 4.6 × 250 mm, 5 μm particle size, Grom, Germany) was used for MC chromatography. A solvent gradient with A (water) and B (acetonitrile), both containing 0.05% trifluoroacetic acid (TFA) (*21*), was established with a flow rate of 1 mL/min. MC-RR and the purified MC-RR variants were diluted in 20% MeOH for chromatographic analysis (determination of purity and quantification), and identified by their respective retention times and characteristic UV absorption spectra.

For quantification of MCs, MC-LR was dissolved in 100% MeOH, diluted in 100% MeOH to a concentration of 10 μM, followed by photometric concentration determination. Each sample was analyzed in triplicates, allowing calculation of the mean absorption. Harada et al. (*22*) reported an identical molar absorption coefficient (ϵ) for MC-LR and MC-RR (ϵ = 39 800 L mol^{-1}cm^{-1}). Lambert−Beer's law allowed calculation of the molar concentration of MC-LR and MC-RR. The molar concentration served to establish a MC-LR standard curve in the RP-HPLC UV-DAD system. Concentrations of [Asp^3]-MC-RR were calculated using standard curve linear regression as no differences in ϵ of MC-LR or MC-RR to [Asp^3]MC-RR are expected based on structure comparison (*22*). For [Asp^3,-Dhb^7]MC-RR an ϵ= 50 400 L mol^{-1}cm^{-1}, established by Blom et al. (*2*), was used. To discriminate between [Asp^3]MC-RR and [Asp^3,Dhb^7]MC-RR synthesized by DS-129, DS-129 extract was spiked with purified [Asp^3,Dhb^7]MC-RR from strain A7 (*2*).

HPLC-ESI-MS/LC/MS. Identification of [Asp^3]MC-RR and [Asp^3,Dhb^7]MC-RR synthesized by DS-129 was achieved by recording mass spectra of the semi-purified MC-RR variants on a combined LC/MS (LCQ Duo mass spectrometer, Finnigan Thermoquest, U.S.) with an electrospray source (ESI-MS). The analysis was performed on a Shimadzu 10AVP system with a photodiode-array detector, a C_{18} reversed-phase column (Grom-Sil 120 ODS-4 HE, 4.6 × 250 mm, 5 μm particle size, Stagroma, Germany), and a flow rate of 1 mL/min. Solvent A (UV-treated deionized water) and solvent B (acetonitrile) were both acidified with 0.05% TFA (Fluka, Switzerland). A linear increase in three steps was applied (solvent B from 30 to 35% in 10 min, 35 to 70% in 30 min, 70−100% in 2 min, isocratic 8 min, (*2*).

Anti-Adda-ELISA. MC standards were analyzed with an anti-Adda-ELISA kit (*23*) in accordance with the manufacturer's instructions (Abraxis, U.S.). The assay was carried out three times in duplicate with MC-RR, [Asp^3]MC-RR, and [Asp^3,Dhb^7]MC-RR. MC-LR was used as the internal standard.

cPPIA. The colorimetric protein-phosphatase-inhibition assay (cPPIA) determines the in vitro inhibitory capacity of MCs and NOD on protein-phosphatase activity (PP1 and PP2A). Tests were carried out with PP1 (rabbit skeletal muscle, recombinant (*E. coli*), New England Biolabs, U.S.) and PP2A (isolated from human red blood cells, V6311, Promega, U.S.) as previously described (*24*). *p*-Nitrophenyl phosphate (*p*NPP, Acros, U.S.) was used as phosphatase substrate. The assay was carried out three times in duplicate with MCs and NOD (see the Supporting Information).

SDS-PAGE, Western Blotting (Anti-PP1 and Anti-Adda). To examine potential covalent binding of MC-LR, MC-RR, [Asp^3]MC-RR, [Asp^3,Dhb^7]MC-RR, and NOD to the catalytic subunit of PP1, MCs and NOD were incubated with PP1 (1 IU per 8 μL enzyme buffer) in enzyme buffer (50 mM Tris Base, 4 mM EDTA, pH 7.0, 1 mM phenylmethylsulphonylfluoride (PMSF), 1 mM benzamidine, 0.2% (v/v) β-mercaptoethanol, 2% (v/v) Triton X-100) at 30 °C for 1.5 h. MCs and NOD (0.5 nmol per 8 μL enzyme buffer) were added in concentrations in excess to PP1 concentration present in the total reaction volume of 30 μL. Three independent replicate experiments were carried out.

To determine the MC-RR-PP1 covalent-binding reaction profile, MC-RR was co-incubated with the catalytic subunit of PP1, using the incubation protocol as already described above. This experiment was carried out in duplicate with seven different incubation times, ranging from 0 min to 16h.

MC-PP1 Protein Complex Sample Preparation. At termination of incubation, MC-PP1 protein complexes were diluted 1:4 with SDS reducing sample buffer (1.5 M Tris Base; pH 8.8, 12.5% (v/v); glycerine, 10% (v/v); 10% SDS solution (w/v), 20% (v/v); β-mercaptoethanol, 5% (v/v), bromphenolblue, 1% (v/v)) and incubated at 95 °C for 5 min. Total protein concentrations were 0.17 units and 0.3 units protein-phosphatase employed for immunostaining with anti-PP1 and anti-Adda antibody (see below). To determine the molecular weight of the detected proteins, a full range recombinant protein molecular weight marker (10, 250 kD) was used (RPN 800, Amersham Pharmacia Biotech, Germany).

SDS-PAGE- Western blotting (PP1 and anti-Adda). Proteins were separated using 10% SDS-Gel electrophoresis (*25*), at room temperature, 200 V and 35 min (Mini-PROTEAN II, Biorad, Germany). Polyacrylamide gels were equilibrated for 30 min in blotting buffer. Subsequently, proteins were blotted semi-dry onto nitrocellulose membranes (PROTRAN, 0.2 μm pore size, Schleicher & Schuell, Germany). Western blotting was carried out in a Mini-PROTEAN II for 90 min at 300 mA and 4 °C. Membranes were blocked in TTBS (Tween Tris buffered saline: 100 mM Tris-HCl, 0.9% NaCl (w/v), 0.1% Tween 20 (v/v)) containing 1% (w/v) bovine serum albumin for 30 min at room temperature. Primary antibodies, rabbit anti-PP1 (IgG fraction of antiserum, P7979, Sigma, Germany) and polyclonal sheep anti-Adda no. 824 (*23*), were both diluted 1:1000 in TTBS. Equilibration was carried out for 60 min. After washing three times (15 min each), membranes were incubated with an alkaline phosphatase-conjugated

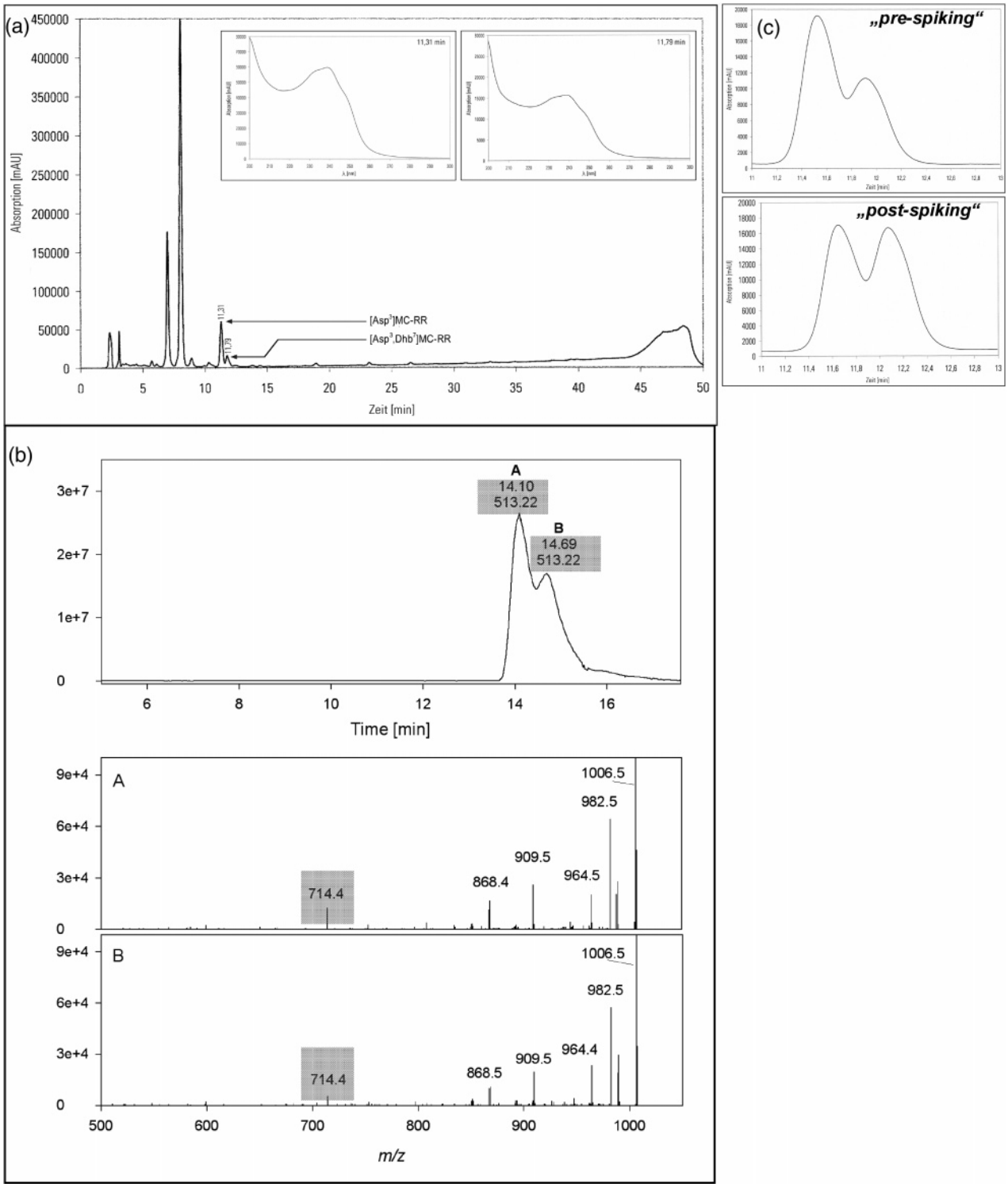

FIGURE 1. Analytical determinations of MC-RR variants in DS-129 extract. (a) HPLC chromatogram: arrows depict [Asp^3]MC-RR and [Asp^3, Dhb^7]MC-RR (inserts show UV-absorption spectra of the two MC-RR variants); (b) LC/MS chromatogram and MS/MS fragmentation spectra of [Asp^3]MC−RR (A) and [Asp^3,Dhb^7]MC−RR (B). Both MCs show fragment ions of $m/z = 714$ representing [Asp^3,Arg^4,Adda^5,Glu^6 + H]$^+$; (c) HPLC chromatograms ($\lambda = 239$ nm) of MC-RR variants pre- and post-spiking with [Asp^3,Dhb^7]MC-RR.

horse anti-rabbit antibody (Roche Biochemicals, Germany) or rabbit anti-sheep antibody (Sigma-Aldrich, Germany) as secondary antibody for 60 min. Membranes were washed three times for 15 min with TTBS and 15 min with TBS (100 mM Tris-HCl, 0.9% NaCl (w/v)). Alkaline phosphatase specific reactions were carried out using FastRed (F-4648, Sigma, Germany) as a substrate, and staining was stopped with purified water.

Results

HPLC-analysis of extracts of the *P. rubescens* culture originally isolated from Lake Ammersee (DS-129) provided for two main MC peaks (Figure 1a). These were identified both by their characteristic UV-spectra (Figure 1a, inserts) and their retention times in comparison to the [Asp^3,Dhb^7]MC-RR standard. The retention times of these two MCs differed only

marginally. Due to insufficient peak separation, the quantification of individual peaks and thus specific variants was imprecise. To confirm the identity of the detected MCs, samples were analyzed by LC/MS. For both MC peaks, double charged ions with the mass of *m*/z 513.2 Dalton $[M+2H]^{2+}$ were observed (Figure 1b). These ions are characteristic for three demethylated MC-RR congeners with the mass of 1023 Dalton, [Asp^3]MC-RR, [Asp^3,Dhb^7]MC-RR, and [Dha^7]MC-RR. To further identify the isolated MCs LC-MS/MS runs were carried out. Both mass spectra showed a significant fragment ion with the mass of m/z 714. This fragment ion may contain [Asp^3, Arg^4, Adda^5, Glu^6 + H]$^+$. Thus, it can be assumed that the MCs of interest are [Asp^3]MC-RR and [Asp^3,Dhb^7]MC-RR, as the fragmentation of [Dha^7]MC-RR would result in a fragment with the mass of m/z 728 [MAsp^3, Arg^4, Adda^5, Glu^6 + H]$^+$. To discriminate between the two MC-RR variants, the extract of the *P. rubescens* strain DS-129 from Lake Ammersee was spiked with purified [Asp^3,Dhb^7]MC-RR from strain A7 (*2*), which resulted in a distinct increase of the second peak (Figure 1c), therefore confirming the presence of [Asp^3,Dhb^7]MC-RR in the second peak.

Quantification of [Asp^3]MC-RR, from strain DS29V, and [Asp^3,Dhb^7]MC-RR, from strain A7, was achieved via analytical HPLC using published MC congener specific absorption coefficients (ϵ,Table 1a). The loss of the methyl group at position 3 in [Asp^3]MC-RR was not considered to have any influence on ϵ. Therefore, $\epsilon = 39\,800\ \mathrm{L\,mol^{-1}cm^{-1}}$ for MC-LR and MC-RR in MeOH (*22*) was used for concentration determinations of [Asp^3]MC-RR. As [Asp^3,Dhb^7]MC-RR has a distinctly different $\epsilon(50\,400\ \mathrm{L\,mol^{-1}cm^{-1}}$, (*2*), the following equation was used for the concentration determination of [Asp^3,Dhb^7]MC-RR via HPLC and MC-LR as standard:

$$c(\mathrm{Asp^3,Dhb^7]MC\text{-}RR}) = c(\mathrm{MC-LR}) \times \epsilon(\mathrm{MC-LR})/\epsilon\ (\mathrm{Asp^3,Dhb^7]MC\text{-}RR})$$

$$= c(\mathrm{MC\text{-}LR}) \times 39\,800/50\,400$$

$$= c(\mathrm{MC\text{-}LR}) \times 0.79 \qquad (1)$$

Concentration determination for [Asp^3,Dhb^7]MC-RR; c = concentration; ϵ = molar absorption coefficient. To support the above quantification results, MC-RR, [Asp^3]MC-RR, and [Asp^3,Dhb^7]MC-RR were also analyzed by anti-Adda-ELISA. The antibody used in this ELISA recognizes the Adda-group of all MC and NOD congeners that contain the Adda side-chain (*23*). Application of congener specific ϵ (*2*, *22*) for concentration determinations resulted in comparable MC-RR variant concentrations (Table 1a) when determined via HPLC-DAD or anti-Adda-ELISA (differences <10%). In contrast, use of an inappropriate $\epsilon(39\,800\ \mathrm{L\,mol^{-1}cm^{-1}})$ for [Asp^3,Dhb^7]MC-RR resulted in an overestimation of the concentration. The MC concentrations as determined via HPLC-DAD (Table 1a) were then used for the ensuing cPPIA experiments and calculation of IC_{50} values.

All tested MC variants and NOD were capable of inhibiting PP1 and 2A (Figure 2a and b). While MC-LR, MC-RR, [Asp^3]-MC-RR, and NOD inhibited PP1 with IC_{50} values in the very low nM range (Table 1b), [Asp^3,Dhb^7]MC-RR inhibited PP1 10- to 20-fold less effectively. With IC_{50} values in the high picomolar range, MC-LR, MC-RR, and [Asp^3]MC-RR are among the most potent PP2A inhibitors known to date (*10*, *24*, *26*), while [Asp^3,Dhb^7]MC-RR, with an IC_{50} value of 29.8 nM, was distinctly less potent. The IC_{50} obtained with NOD was similar for both PP1 and 2A (Table 1b).

The covalent binding potential of MC-LR, MC-RR, [Asp^3]-MC-RR, [Asp^3,Dhb^7]MC-RR, and NOD to the catalytic subunit of PP1 was analyzed via in vitro incubation and Western blotting using antibodies against the catalytic subunit of PP1 and the Adda-group of MCs and NODs (Figure 2c), respectively. MC-RR, [Asp^3]MC-RR, and MC-LR incubations, whether identified with anti-PP1 or the anti-Adda antibody, presented with a protein band corresponding to a molecular weight of 34 kDa. In contrast, [Asp^3,Dhb^7]MC-RR and NOD-incubations presented with an anti-PP1 positive protein band corresponding to a molecular weight of 33kDa, while no anti-Adda positive bands were detectable, suggesting that neither [Asp^3,Dhb^7]MC-RR nor NOD bound covalently to PP1. MC-RR was incubated for up to 16 h with PP1 in order to investigate whether or not covalent binding of MC-RR to PP1 is incubation time dependent. This experiment demonstrated that, although MC-RR covalently bound to PP1 within seconds of incubation (Figure 2d), the intensity of the bands increased with the duration of the incubation. Spontaneous formation of covalent bonds during Western blotting could be excluded by addition of a SDS denatured PP1-MC-RR mixture and incubated for 16 h, which also gave negative results with anti-Adda antibodies (data not shown). NOD and [Asp^3,Dhb^7]MC-RR were also incubated for up to 16 h with PP1 in order to investigate whether covalent binding of NOD and [Asp^3,Dhb^7]MC-RR to PP1 was not detected due to restrictions in reaction time. However, no difference in

TABLE 1. Comparison of Quantification Results of MC-RR, [Asp]MC-RR, and [Asp^3,Dhb^7]MC-RR; (a) via Anti-Adda-ELISA and HPLC-DAD; and (b) via Comparison of IC_{50} and LD_{50} (mice, i.p.) Values of Various Dhb^7-containing MCs, MC-LR, MC-RR, and NOD[a]

	(a)	
MC-variants	anti-Adda-ELISA (μM)	HPLC-DAD (μM)
MC-RR	0.60 ± 0.06	0.62 ± 0.03 ($\epsilon = 39\,800\ \mathrm{L\,mol^{-1}\,cm^{-1}}$)
[Asp^3]MC-RR	0.63 ± 0.14	0.64 ± 0.01 ($\epsilon = 39\,800\ \mathrm{L\,mol^{-1}\,cm^{-1}}$)
[Asp^3, Dhb^7]MC-RR	0.53 ± 0.05	0.65 ± 0.01 ($\epsilon = 39\,800\ \mathrm{L\,mol^{-1}\,cm^{-1}}$) 0.50 ± 0.01 ($\epsilon = 50\,400\ \mathrm{L\,mol^{-1}\,cm^{-1}}$)

	(b) IC_{50}(nM)		
congener	PP1	PP2A	LD_{50} (nmol/kg bw)
MC-LR	2.5 (1.7−3.7) 0.25[b] 0.2[c]	0.68 (0.64−0.74) 0.05[b] 0.05−0.08[c] 0.3[d]	33−73[e]
MC-RR	1.9 (1.3−3.0) 0.68[b]	0.75 (0.59−0.96) 0.1[b]	580−630[f]
[Asp^3,Dhb^7]-MC-RR	56.4 (27.3−116.5) 1.8[b]	29.8 (17.9−49.4) 2.4[b]	250[g] 400[j]
[Asp^3]MC-RR	3.8 (2.6−5.7)	0.45 (0.34−0.61)	250[h]
[D-Asp^3,(*E*)-Dhb^7]MC-LR	nd	nd	70[g]
[D-Asp^3,(*E*)-Dhb^7]MC-HtyR	nd	nd	70[g]
[D-Asp^3,(*E*)-Dhb^7]MC-HilR	nd	0.3[d]	nd
[D-Asp^3, ADMAdda^5,(*E*)-Dhb^7]MC-HtyR	0.15−0.24[c]	0.06[c]	100[j]
[D-Asp^3, ADMAdda^5,(*E*)-Dhb^7]MC-RR	nd	nd	200[j]

[a] IC_{50} (cPPIA) values determined in this study are given in nM (95% CI). [b] fluorimetric PPA (*36*). [c] Radioactive PPA (*10*). [d] Fluorimetric PPA (*37*). [e] Refs *42*−*44*. [f] Refs *44*−*45*. [g] Ref *32*. [h] Ref *27*. [i] Ref *46*. [j] Ref *31*, LD_{100}. [k] Ref *47*; nd is no data available; PP Source, PP2A; Human Red Blood Cells (this study and ref *37*; rabbit skeletal muscle (*36*); bovine heart (*10*); PP1, rabbit skeletal muscle; recombinant (*E. coli*), this study and refs *10, 36*.

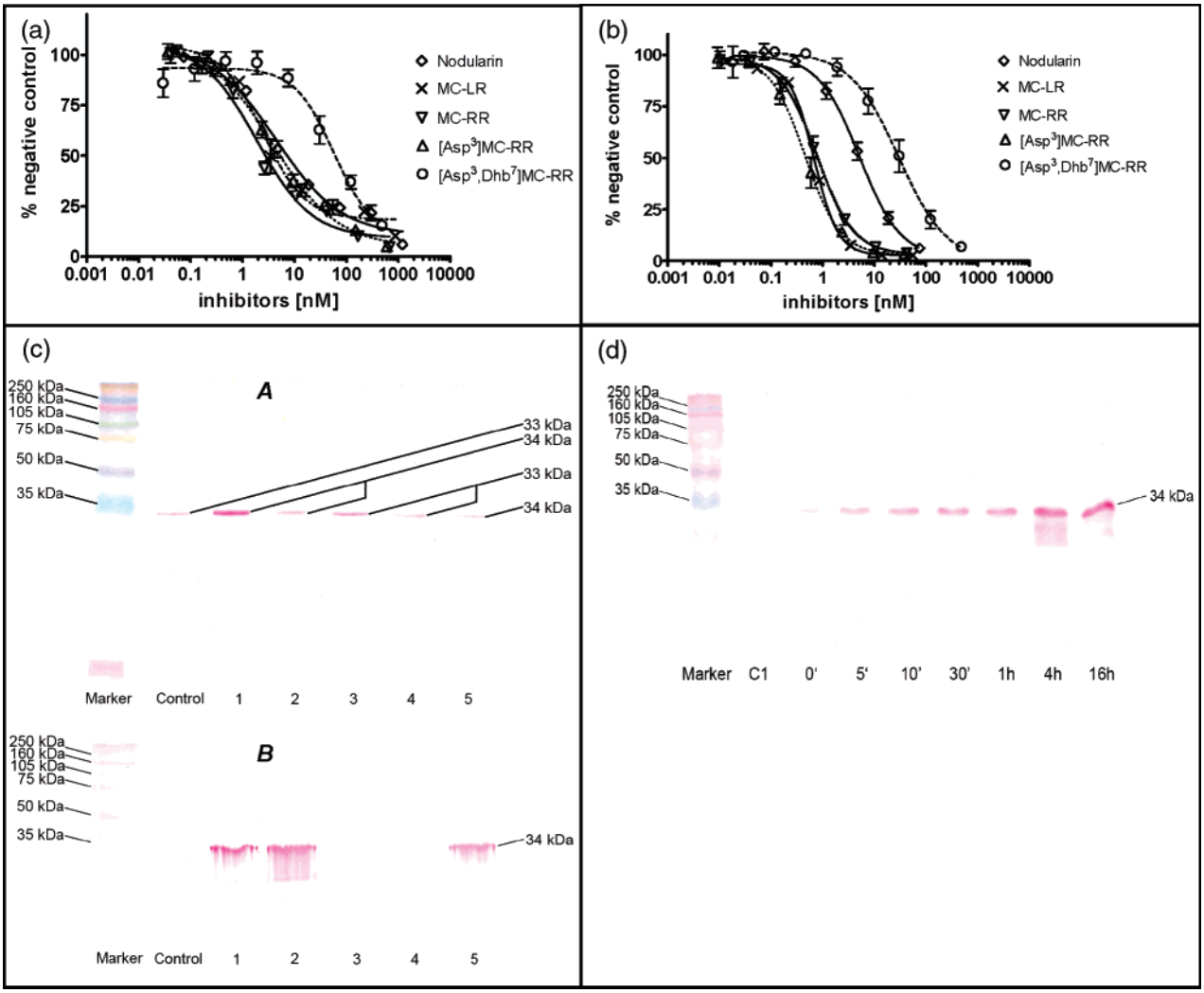

FIGURE 2. Inhibition of protein phosphatases (PPIA) and covalent protein binding (Western blot) by MCs and NOD. (a) PPIA with PP1; (b) PPIA with PP2A (percent negative control is equivalent to percent activity of PP without inhibitor. Values represent mean ± standard error of the mean of three replicate analyses); (c) western blot following 1.5 h incubation of MCs and NOD with the catalytic subunit of PP1 and detection with (A) anti-PP1 antibody and (B) anti-Adda antibody. Lanes: marker protein, control (PP1 without MC or NOD), (*1*) PP1+MC-RR, (*2*) PP1+[Asp^3]MC-RR, (*3*) PP1+[Asp^3,Dhb^7]MC-RR, (*4*) PP1+NOD, and (*5*) PP1+MC-LR; (d) Western blot following varying incubation times of MC-RR with the catalytic subunit of PP1, and detection with anti-Adda antibody. Lanes: Marker; (C1) PP1 without MC-RR; 0′, 5′, 10′, 30′, 1 h, 4 h, 16 h: incubation periods of PP1 with MC-RR.

the 1.5 h incubation result could be detected (data not shown), i.e., lack of covalent binding to PP1 was confirmed.

Discussion

RP-HPLC-DAD and LC/MS analyses of an extract of an unialgal culture of *P. rubescens* isolated from Lake Ammersee (DS-129) demonstrated that primarily two MCs with the mass of *m*/z 1024 $[M + H]^+$ are synthesized by this strain. Three MCs with the same mass (1023 Da) resulting in double charged quasi-molecular ions with m/z 513 $[M + H]^{2+}$ in the LC/MS analyses have been previously reported, i.e., [Asp^3]-MC-RR (*27*−*28*), [Dha^7]MC-RR (*28*−*30*), and [D-Asp^3,(*E*)-Dhb^7]MC-RR (*2*, *31*, *32*). The DS-129 extract was deemed not to contain [Dha^7]MC-RR as this congener does not produce a fragment ion with the mass of m/z 714, which was the prominent fragment in the MS/MS analysis of the DS-129 extract. Additional spiking of the DS-129 extract with a purified [Asp^3, Dhb^7]MC-RR standard confirmed synthesis of [Asp^3]MC-RR and Asp^3,Dhb^7]MC-RR by DS-129.

Due to the high number of MC congeners (most likely >80, ref *33*), the broad spectrum of their chemical properties and the lack of analytical standards, accurate quantification of single MCs is problematic. One of the currently acceptable methods is the photometric determination using HPLC-DAD. However, photometric determination depends on the accuracy and availability of the respective absorption coefficients (ϵ). Indeed, the $\epsilon$of [Asp^3,Dhb^7]MC-RR (*2*) and MC-LR/MC-RR (*22*) differ substantially, which potentially leads to an overestimation of the concentration of [Asp^3,Dhb^7]MC-RR if the concentration of [Asp^3,Dhb^7]MC-RR is calculated using MC-LR or MC-RR as standards (Table 1a). Using MC-LR or MC-RR standard curves for quantification is, however, possible if a correction factor is introduced, as demonstrated in eq 1. Indeed, the comparison of quantification of [Asp^3,-Dhb^7]MC-RR via HPLC-DAD (including correction factor) and via anti-Adda-ELISA demonstrated high determination consistency.

The MC-LR and MC-RR IC_{50} values determined with the cPPIA (Table 1b) are in agreement with previously published values achieved with comparable assays (*34*, *35*). The distinctly higher IC_{50} values for [Asp^3,Dhb^7]MC-RR corroborate earlier reports by Blom et al. (*36*) using a fluorescent PPIA substrate with PP1 and PP2A.

In a study by Rapala et al. (*20*), the concentration of [Asp^3]-MC-RR (isolated from strains from Finnish lakes) measured with the PPIA (using PP1) were only 5% of that determined by ELISA and HPLC. As demonstrated here, it is very difficult to distinguish between [Asp^3]MC-RR and [Asp^3,Dhb^7]MC-RR based on analyses using retention time, UV-spectra, and low-resolution mass spectra. Therefore, it is possible that [Asp^3,Dhb^7]MC-RR was one or even the predominant MC congener present in the sample analyzed by Rapala et al. (*20*), which would explain the discrepancy between the ELISA, HPLC, and the PPIA data reported. However, as NMR-studies and/or standards are essential to indiscriminately identify [Asp^3,Dhb^7]MC-RR, which were not available to Rapala et al. (*20*), the latter interpretation cannot be corroborated. Thus the observation that quantification of MCs by HPLC-DAD and ELISA differ distinctly from quantification results obtained via PPIAs may be explained in part by MC congener inherent differences in PP inhibitory capacity. However, as not all PPIAs reported employed the same PP source (native tissue PP preparations of different tissue or animal origin or recombinant PPs), some of the differences observed among the PP inhibitory capacity of MC congeners may also be due to methodical variations and artifacts (Table 1b). The latter observations highlight the problems associated with the routine use of the PPIA to determine MC and NOD concentration measurements in water and cyanobacterial extract samples.

Moreover, it must be taken into account that the PPIA determines only the PP inhibition potential of a given sample and, therefore, only the sum of all PP inhibiting MCs in this sample. As it cannot a priori be assumed that the more than 80 different MC congeners inhibit PPs equally, as exemplified by the comparison of the PP1 and 2A inhibiting capacity of MC-RR and [Asp^3,Dhb^7]MC-RR in the study here, the results obtained with PPIAs may severely underestimate the actual MC concentrations present. However, not all Dhb^7-containing MC congeners demonstrate weaker PP inhibition capacity. Indeed, neither [D-Asp^3,(*E*)-Dhb^7]MC-HilR (*37*) nor [D-Asp^3,(*E*)-Dhb^7]MC-HtyR (*10*) were observed to have lower PP inhibitive activity than corresponding concentrations of MC-LR (Table 1b). Conversely, other non-MC or -NOD PP inhibitors present in water or bloom samples analyzed via PPIA may wrongly suggest the presence of PP inhibiting MCs or NOD. Thus the results of the cPPIA provide a mere estimate of PP-inhibiting potential but no proof of MC or NOD presence nor any information on the MC or NOD congeners present.

The results presented here in conjunction with evidence published earlier (*10*) suggest that MC congeners lacking a MDha on position 7 do not covalently bind to PPs. This pertains not only to Dhb^7 MCs, but also to MCs with an alanine or serine at position 7 (summarized in Kaya et al. (*38*)). Despite that this study demonstrated that [Asp^3,Dhb^7]-MC-RR does not covalently bind to the catalytic subunit of PP1 in vitro (Figure 2c), and a similar observation was reported for [D-Asp^3,(*E*)-Dhb^7]MC-HtyR by Hastie et al. (*10*), the Dhb at position 7 and, therefore the lack of covalent binding capability to PPs, does not a priori explain the weaker inhibition of the PPs, especially as no weaker PP inhibition was reported for Dhb^7-containing [D-Asp^3,(*E*)-Dhb^7]MC-HilR (*37*) and [D-Asp^3,(*E*)-Dhb^7]MC-HtyR (*10*). From the currently available data it is thus hypothesized that the combination of the two arginines at positions 2 and 4 with Dhb at position 7 may be sterically hindering and thus restrict binding of [Asp^3,Dhb^7]MC-RR to the catalytic subunit of the PP.

The numerous variations in amino acid composition and thus high number of MC congeners is of great concern, especially when in vivo acute toxicity data are the sole information available and chronic data are scarce or absent. The consequence is that for better understanding of potential risk acute in vivo data is compared to mechanistic in vitro data. Indeed, no difference in the LD_{50} values (mice, i.p.) can be observed for [Asp^3]MC-RR (*27*) and [D-Asp^3,(*E*)-Dhb^7]MC-RR (*32*). Furthermore, [D-Asp^3,(*E*)-Dhb^7]MC-RR was shown to be more toxic to invertebrates (on the basis of LC_{50} values) than MC-LR or NOD (*2*). These observations suggest that the PP inhibiting capacity and the ability to form covalent bonds to enzymes of the PP family do not consistently explain the observed in vivo toxicity and thus are a poor measure of potential risk. Furthermore, although the LD_{50} values of MC-LR and [D-Asp^3,(*E*)-Dhb^7]MC-LR differed only marginally (Table 1b), mice were treated once per week (i.p.) for 14 months with [D-Asp^3,(*E*)-Dhb^7]MC-LR presented with a distinctly reduced liver tumor incidence than mice treated with MC-LR (*39*, *40*). Whether a lower PP inhibiting capacity (toxicodynamics) or reduced biological availability (toxicokinetics) of [D-Asp^3,(*E*)-Dhb^7]MC-LR is decisive for liver tumor promotion is yet to be determined. Consequently, the presence of a Dhb group in a given MC congener, and therefore the lack of covalent binding to PPs, may be indicative for the tumor-promoting capacity of individual MCs, but not for its acute toxicity.

The current risk assessment model for MC exposure is based entirely on toxicokinetic and -dynamic properties of MCs and especially on the subchronic toxicity of MC-LR (*8*, *41*). Drinking water/recreational water guideline values are then calculated based on MC-LR equivalents, primarily calculated based on the PP inhibiting potential of the different congeners. Although PPs are assumed to be the primary target for MCs and NODs, the caveats of determining PP inhibitory capacity as a measure of potential in vivo toxicity must be kept in mind. Indeed, it is becoming more apparent that the PP inhibiting capacity of most MCs is not directly correlated with their respective in vivo toxicity (based on LD_{50} values).

Therefore, the PP inhibiting potencies presented here when compared to the in vivo data available, strongly suggest that MC congeners can differ profoundly in their toxicodynamic and -kinetic properties and, therefore, emphasize, as suggested by Dietrich and Hoeger (*8*) earlier, that the risk assessment schemes based on MC-LR equivalents are insufficient.

Acknowledgments

Parts of this project were funded by the EU (QLRT-2001-02634, D.R.D. and S.H.) and the Arthur-and-Aenne-Feindt Foundation (D.R.D., B.E., and D.S.). Thanks to Dr. Evelyn O'Brien and to Prof. Dr. F. Jüttner for helpful comments and for valuable discussions. S.J.H. and D.S. contributed equally to this work.

Supporting Information Available

Further details about the chemicals and strains used in the experiment, a schematic of the experiment, and information about the sampling and cultivation of cyanobacteria. This material is available free of charge via the Internet at http://pubs.acs.org.

Literature Cited

(1) Skulberg, O. M.; Codd, G. A.; Carmichael, W. W. Toxic blue-green algal blooms in Europe: A growing problem. *Ambio* **1984**, *13*, 244−247.

(2) Blom, J. F.; Robinson, J. A.; Jüttner, F. High grazer toxicity of [D-Asp^3,(*E*)-Dhb^7]microcystin-RR of *Planktothrix rubescens* as compared to different microcystins. *Toxicon* **2001**, *39*, 1923−1932.

(3) Kurmayer, R.; Christiansen, G.; Fastner, J.; Börner, T. Abundance of active and inactive microcystin genotypes in populations of the toxic cyanobacterium *Planktothrix* spp. *Environ. Microbiol.* **2004**, *6*, 831−841.

(4) Fastner, J.; Erhard, M.; Carmichael, W. W.; Sun, F.; Rinehart, K. L.; Roenicke, H.; Chorus, I. Characterization and diversity of

microcystins in natural blooms and strains of the genera Microcystis and Planktothrix from German freshwaters. *Arch. Hydrobiol.* **1999**, *145*, 147−163.
(5) Ernst, B.; Hitzfeld, B.; Dietrich, D. Presence of *Planktothrix* sp. and cyanobacterial toxins in Lake Ammersee, Germany and their impact on whitefish (*Coregonus lavaretus* L.). *Environ. Toxicol.* **2001**, *16*, 483−488.
(6) Annila, A.; Lehtimaki, J.; Mattila, K.; Eriksson, J. E.; Sivonen, K.; Rantala, T. T.; Drakenberg, T., Solution structure of nodularin. An inhibitor of serine/threonine- specific protein phosphatases. *J. Biol. Chem.* **1996**, *271*, 16695−16702.
(7) Kaebernick, M.; Neilan, B. A. Ecological and molecular investigations of cyanotoxin production. *FEMS Microbiol. Ecol.* **2001**, *35*, 1−9.
(8) Dietrich, D. R.; Hoeger, S. J. Guidance values for microcystins in water and cyanobacterial supplement products (blue-green algal supplements): a reasonable or misguided approach? *Toxicol. Appl. Pharmacol.* **2005**, *203*, 273−289.
(9) Fischer, W. J.; Altheimer, S.; Cattori, V.; Meier, P. J.; Dietrich, D. R.; Hagenbuch, B. Organic anion transporting polypeptides expressed in liver and brain mediate uptake of microcystin. *Toxicol. Appl. Pharmacol.* **2005**, *203*, 257−263.
(10) Hastie, C. J.; Borthwick, E. B.; Morrison, L. F.; Codd, G. A.; Cohen, P. T. Inhibition of several protein phosphatases by a non-covalently interacting microcystin and a novel cyanobacterial peptide, nostocyclin. *BBA* **2005**, *1726*, 187−193.
(11) Eriksson, J. E.; Paatero, G. I. L.; Meriluoto, J. A. O.; Codd, G. A.; Kass, G. E. N.; Nicotera, P.; Orrenius, S. Rapid microfilament reorganization induced in isolated rat hepatocytes by microcystin-LR, a cyclic peptide toxin. *Exp. Cell Res.* **1989**, *185*, 86−100.
(12) Ohta, T.; Sueoka, E.; Iida, N.; Komori, A.; Suganuma, M.; Nishiwaki, R.; Tatematsu, M.; Kim, S. J.; Carmichael, W. W.; Fujiki, H. Nodularin, a potent inhibitor of protein phosphatases 1 and 2A, is a new environmental carcinogen in male F344 rat liver. *Cancer Res.* **1994**, *54*, 6402−6406.
(13) Grosse, Y.; Baan, R.; Straif, K.; Secretan, B.; El Ghissassi, F.; Cogliano, V. Carcinogenicity of nitrate, nitrite, and cyanobacterial peptide toxins. *Lancet Oncol.* **2006**, *7*, 628−629.
(14) MacKintosh, R. W.; Dalby, K. N.; Campbell, D. G.; Cohen, P. T.; Cohen, P.; MacKintosh, C. The cyanobacterial toxin microcystin binds covalently to cysteine-273 on protein phosphatase 1. *FEBS Lett.* **1995**, *371*, 236−240.
(15) Craig, M.; Luu, H. A.; McCready, T. L.; Williams, D.; Andersen, R. J.; Holmes, C. Molecular mechanisms underlying the interaction of motuporin and microcystins with type-1 and type-2A protein phosphatases. *Biochem. Cell Biol.* **1996**, *74*, 569−578.
(16) Bagu, J. R.; Sönnichsen, F. D.; Williams, D.; Andersen, R. J.; Sykes, B. D.; Holmes, C. F. B. Comparison of the solution structures of microcystin-LR and motuporin [letter]. *Nat. Struct. Biol.* **1995**, *2*, 114−116.
(17) Goldberg, J.; Huang, H. B.; Kwon, Y. G.; Greengard, P.; Nairn, A. C.; Kuriyan, J. Three-dimensional structure of the catalytic subunit of protein serine/threonine phosphatase-1. *Nature* **1995**, *376*, 745−753.
(18) Bagu, J. R.; Sykes, B. D.; Craig, M. M.; Holmes, C. A molecular basis for different interactions of marine toxins with protein phosphatase-1—Molecular models for bound motuporin, microcystins, okadaic acid, and calyculin A. *J. Biol. Chem.* **1997**, *272*, 5087−5097.
(19) Ernst, B.; Hoeger, S. J.; O'Brien, E.; Dietrich, D. R. Oral toxicity of the microcystin-containing cyanobacterium *Planktothrix rubescens* in European whitefish (*Coregonus lavaretus*). *Aquat. Toxicol.* **2006**, *79*, 31−40.
(20) Rapala, J.; Erkomaa, K.; Kukkonen, J.; Sivonen, K.; Lahti, K. Detection of microcystins with protein phosphatase inhibition assay, high-performance liquid chromatography-UV detection and enzyme-linked immunosorbent assay; Comparison of methods. *Anal. Chim. Acta* **2002**, *466*, 213−231.
(21) Lawton, L. A.; Edwards, C.; Codd, G. A. Extraction and high-performance liquid-chromatographic method for the determination of microcystins in raw and treated waters. *Analyst* **1994**, *119*, 1525−1530.
(22) Harada, K.; Ogawa, K.; Matsuura, K.; Murata, H.; Suzuki, M.; Watanabe, M. F.; Itezono, Y.; Nakayama, N. Structural determination of geometrical isomers of microcystins LR and RR from cyanobacteria by two-dimensional NMR spectroscopic techniques. *Chem. Res. Toxicol.* **1990**, *3*, 473−481.
(23) Fischer, W. J.; Garthwaite, I.; Miles, C. O.; Ross, K. M.; Aggen, J. B.; Chamberlin, A. R.; Towers, N. R.; Dietrich, D. R. Congener-independent immunoassay for microcystins and nodularins. *Environ. Sci. Technol.* **2001**, *35*, 4849−4856.
(24) Heresztyn, T.; Nicholson, B. C. Determination of cyanobacterial hepatotoxins directly in water using a protein phosphatase inhibition assay. *Water Res.* **2001**, *35*, 3049−3056.
(25) Laemmli, U. Cleavage of structural proteins during assembly of the head of bacteriphage T4. *Nature* **1970**, *227*, 680−685.
(26) MacKintosh, C.; Beattie, K. A.; Klumpp, S.; Cohen, P.; Codd, G. A. Cyanobacterial microcystin-LR is a potent and specific inhibitor of protein phosphatases 1 and 2A from both mammals and higher plants. *FEBS Lett.* **1990**, *264*, 187−192.
(27) Meriluoto, J. A. O.; Sandström, A.; Eriksson, J. E.; Remaud, G.; Craig, A. G.; Chattopadhyaya, J. Structure and toxicity of a peptide hepatotoxin from the cyanobacterium *Oscillatoria agardhii*. *Toxicon* **1989**, *27*, 1021−1034.
(28) Sivonen, K.; Namikoshi, M.; Evans, W. R.; Carmichael, W. W.; Sun, F.; Rouhiainen, L.; Luukkainen, R.; Rinehart, K. L. Isolation and characterization of a variety of microcystins from seven strains of the cyanobacterial genus *Anabaena*. *Appl. Environ. Microbiol.* **1992**, *58*, 2495−2500.
(29) Kiviranta, J.; Namikoshi, M.; Sivonen, K.; Evans, W. R.; Carmichael, W. W.; Rinehart, K. L. Structure determination and toxicity of a new microcystin from *Microcystis aeruginosa* strain 205. *Toxicon* **1992**, *30*, 1093−1098.
(30) Luukkainen, R.; Namikoshi, M.; Sivonen, K.; Rinehart, K.; Niemelä, S. Isolation and identification of 12 microcystins from four strains and two bloom samples of *Microcystis* spp.: structure of a new hepatotoxin. *Toxicon* **1994**, *32*, 133−139.
(31) Sano, T.; Kaya, K. A 2-amino-2 butenoic acid (Dhb)-containing microcystin isolated from *Oscillatoria agardhii*. *Tetrahedron Lett.* **1995**, *36*, 8603−8606.
(32) Sano, T.; Kaya, K. Two new (E)-2-Amino-2-Butenoic Acid (Dhb)-Containing Microcystins isolated from *Oscillatoria agardhii*. *Tetrahedron* **1998**, *54*, 463−470.
(33) Spoof, L. Microcystins and nodularins. In *Toxic—Cyanobacterial Monitoring and Cyanotoxin Analysis*; Meriluoto, J., Codd, G. A., Eds.; Abo Akademi University Press: Turku, 2005; Vol. 65, pp 15−40.
(34) Rivasseau, C.; Racaud, P.; Deguin, A.; Hennion, M. C., Development of a bioanalytical phosphatase inhibition test for the monitoring of microcystins in environmental water samples. *Anal. Chim. Acta* **1999**, *394*, 243−257.
(35) Robillot, C.; Hennion, M. C. Issues arising when interpreting the results of the protein phosphatase 2A inhibition assay for the monitoring of microcystins. *Anal. Chim. Acta* **2004**, *512*, 339−346.
(36) Blom, J. F.; Jüttner, F. High, crustacean toxicity of microcystin congeners does not correlate with high protein phosphatase inhibitory activity. *Toxicon* **2005**, *46*, 465−470.
(37) Sano, T.; Takagi, H.; Kaya, K. A Dhb-microcystin from the filamentous cyanobacterium *Planktothrix rubescens*. *Phytochemistry* **2004**, *65*, 2159−2162.
(38) Kaya, K.; Sano, T.; Inoue, H.; Takagi, H. Selective determination of total normal microcystin by colorimetry, LC/UV detection and/or LC/MS. *Anal. Chim. Acta* **2001**, *450*, 73−80.
(39) Ichinose, T.; Sano, T.; Sadakane, K.; Kawazato, H.; Kaya, K. Promoting and progressive effects of [D-Asp^3,(*E*)-Dhb^7]Microcystin-LR and Microcystin-LR on the development of spontaneous liver tumour in C3H/HEN mice. In *Abstract book of the 10th Conference on Harmful Algae, X- Harmful Algae Blooms*; Steidinger, K. A., Landsberg, J. H., Tomas, C. R., Vargo, G. A., Eds.; UNECSO: Florida, 2002; Vol. 1, p 136.
(40) Sano, T.; Takagi, H.; Sadakane, K.; Ichinose, T.; Kawazato, H.; Kaya, K. Carcinogenic effects of microcystin-LR and Dhb-microcystin-LR on mice liver. In Abstract book of the *6th International Conference on Toxic Cyanobacteria*, Bergen, Norway, 2004; p 59.
(41) Kuiper-Goodman, T.; Falconer, I. R.; Fitzgerald, D. J. Human Health Aspects. In *Toxic Cyanobacteria in Water: A Guide to their Public Health Consequences, Monitoring and Management*; Chorus, I., Bartram, J., Eds.; E & FN Spon: London, 1999.
(42) Krishnamurthy, T.; Carmichael, W. W.; Sarver, E. W. Toxic peptides form freshwater cyanobacteria (blue-green algae). I. Isolation, purification and characterization of peptides from Microcystis aeruginosa and Anabaena flos-aquae. *Toxicon* **1986**, *24*, 865−873.
(43) Lovell, R. A.; Schaeffer, D. J.; Hooser, S. B.; Haschek, W. M.; Dahlem, A. M.; Carmichael, W. W.; Beasley, V. R. Toxicity of intraperitoneal doses of microcystin-LR in two strains of male mice. *J. Environ. Pathol., Toxicol. Oncol.* **1989**, *9*, 221−237.

(44) Stoner, R.; Adams, W.; Slatkin, D.; Siegelman, H. The effects of single L-amino acid substitutions on the lethal potencies of the microcystins. *Toxicon* **1989**, *27*, 825−828.

(45) Watanabe, M. F.; Oishi, S.; Harada, K.; Matsuura, K.; Kawai, H.; Suzuki, M. Toxins contained in *Microcystis* species of cyanobacteria (blue-green algae). *Toxicon* **1988**, *26*, 1017−1025.

(46) Beattie, K. A.; Kaya, K.; Sano, T.; Codd, G. A. Three dehydrobutyrine-containing microcystins from Nostoc. *Phytochemistry* **1998**, *47*, 1289−1292.

(47) Eriksson, J. E.; Meriluoto, J. A.; Kujari, H. P.; Osterlund, K.; Fagerlund, K.; Hallbom, L. Preliminary characterization of a toxin isolated from the cyanobacterium *Nodularia spumigena*. *Toxicon* **1988**, *26*, 161−166.